

PAPER • OPEN ACCESS

High temperature magnetic characterisation of structural steels using Epstein frame

To cite this article: John W Wilson *et al* 2021 *Meas. Sci. Technol.* **32** 125601

View the [article online](#) for updates and enhancements.

You may also like

- [ICRU Report 64: Dosimetry of High-Energy Photon Beams Based on Standards of Absorbed Dose to Water](#)
D W O Rogers
- [The Earth radiation balance as driver of the global hydrological cycle](#)
Martin Wild and Beate Liepert
- [Summary](#)
F Hensel

High temperature magnetic characterisation of structural steels using Epstein frame

John W Wilson^{1,*} , Lei Zhou², Claire L Davis² and Anthony J Peyton¹

¹ Department of Electrical and Electronic Engineering, The University of Manchester, Sackville Street Building, Manchester M1 3BU, United Kingdom

² WMG, International Manufacturing Centre, University of Warwick, Coventry CV4 7AL, United Kingdom

E-mail: john.wilson@manchester.ac.uk

Received 25 May 2021, revised 6 July 2021

Accepted for publication 27 July 2021

Published 23 August 2021



CrossMark

Abstract

Electromagnetic non-destructive testing techniques provide an attractive solution to the problem of monitoring microstructural changes in steels undergoing heat treatment as they are non-contact, have a short response time and are relatively inexpensive. However, to take full advantage of these techniques it is necessary to be able accurately measure the magnetisation characteristics of the materials of interest at temperatures up to the Curie point. This paper details the development of a novel high temperature Epstein frame for installation in a furnace with the design informed and results validated by finite element modelling. Hysteresis loop characteristics are successfully measured for a dual phase steel up to the Curie point for heating and cooling. Results show the developed system has the potential to provide valuable data to inform online electromagnetic monitoring systems.

Keywords: Epstein frame, magnetic hysteresis, steel, BH measurement, high temperature

(Some figures may appear in colour only in the online journal)

1. Introduction

In steel processing, metallurgists design and control thermal-mechanical and/or thermal processing parameters, such as reduction ratio, temperature, and time, to carefully develop desired microstructures which define the mechanical properties of the final product. It would be hugely beneficial to monitor and characterise microstructural changes on-line during processing, allowing in-situ feedback control through non-destructive methods.

A number of NDT techniques such as x-ray, electromagnetic and laser ultrasonic sensors [1–3] have been developed for this purpose, each of them with their own advantages and shortcomings. Electromagnetic (EM) techniques have attracted much attention for monitoring microstructure changes below Curie point due to their advantages of being non-contact, having a short response time and being relatively inexpensive [4–7].

Commercial EM sensor systems such as EMspecTM [4], operating at a low applied magnetic field, exploit the differences in relative permeability and electrical conductivity, between different microstructural phases to provide information on the transformed fraction. EMspecTM is used on-line, on the run-out table of a hot strip mill to detect and monitor phase transformation, with the steel being at high temperatures (typically 500 °C–750 °C) and the sensor positioned below the hot steel and being water cooled [5].

* Author to whom any correspondence should be addressed.



Original Content from this work may be used under the terms of the [Creative Commons Attribution 4.0 licence](https://creativecommons.org/licenses/by/4.0/). Any further distribution of this work must maintain attribution to the author(s) and the title of the work, journal citation and DOI.

If EM inspection systems are to be accepted in hot steel processing environments, including in-situ in heat treatment furnaces, greater understanding of the results and therefore greater confidence in these types of systems can be gained by developing a full understanding of the induction versus field strength (BH) characteristics of the specific structural steels being processed at a range of temperatures up to the Curie point.

The Epstein frame provides a standardised method for the characterisation of the magnetic properties and calculation of magnetic losses for soft magnetic materials such as grain oriented or non-oriented electrical steels according to international standards IEC 60404-2 [8, 9]. The Epstein frame consists of a primary winding and a secondary winding with the samples to be tested inserted in these windings acting as a core. This arrangement forms an unloaded transformer from which the magnetic properties of the samples can be measured. The samples to be tested are arranged into a square, usually with four samples per side with overlapping corner joints, forming a closed magnetic circuit. The dimensions of the steel strips are standardised at 280 mm × 30 mm × sample thickness. By measuring the current applied to the primary via a current sense resistor the applied field can be calculated. By measuring the induced current of the secondary winding, the magnetic inductance can be measured [6].

Although Epstein frame measurements carried out in accordance with IEC standards offer an excellent framework for accurate, repeatable assessment of a material's magnetic properties, the limitations imposed by testing at high temperatures demand that a more pragmatic approach be taken. There have been numerous attempts to implement this in recent years. Foster [10] measured the core losses and hysteresis losses of oriented silicon steels at 60 Hz up to a maximum temperature of 200 °C using a standard Epstein frame configuration. Messal *et al* [11] measured full BH loops on NiFe 80/20 alloy at 0.5 Hz up to 338 °C with a relatively low applied field of 80 A m⁻¹, though little detail is given regarding the measurement apparatus. Mouillet *et al* and Akroune *et al* [12, 13] measured the magnetic properties of non-oriented electrical steels at frequencies of 50 Hz–2000 Hz using a modified Epstein frame up to a maximum temperature of 220 °C. The effects of excitation frequency, temperature, and strip angle with respect to rolling direction on the measured magnetic properties of grain oriented electrical steel using both full sized and miniaturised frame configurations were investigated by Cheng *et al* [14] at a relatively low temperature of 125 °C. A much higher temperature of 600 °C was reached by Ababsa *et al* [15]: a full sized frame constructed according to IEC 60404-2 [8] was used, built on a ceramic former with nickel coated copper wires employed to avoid oxidation. Magnetic measurements were carried out on grain-oriented electrical steel in the 30–400 Hz frequency range with a relatively low applied field of around 500 A m⁻¹.

The BH characteristics of a variety of steels, including structural steels, have been studied up to temperatures of 800 °C by utilising toroidal samples wrapped with insulated primary and secondary windings, also known as a Rowland ring [16–20]. Although this arrangement can provide accurate magnetic

measurements, and eliminates systematic errors associated with Epstein frame measurements due to the inhomogeneity of the magnetic circuit caused by the double overlapping corners [21], new measurement apparatus must be constructed for each material of interest. For comparative studies on a range of materials, this would be a laborious process with the potential to introduce errors through difficulties in sample machining, inconsistencies in coil winding, etc.

In contrast to much of the work carried out using Epstein frames, the aim of the work described in this paper is the characterisation of the magnetic properties of structural steels. This brings an additional set of requirements to the design of the equipment. Firstly, low frequency (≤ 1 Hz) excitation must be employed to minimise the influence of eddy currents and allow the user to derive the true BH characteristics of the material. To do this, primary coils with many more windings than those used for their higher frequency (≥ 30 Hz) counterparts must be employed. Secondly, a higher applied field of several kA m⁻¹ is needed to drive magnetically harder structural steels close to saturation than is needed for the much magnetically softer electrical steels commonly studied in these types of tests. The remainder of this paper details the construction of a novel high temperature Epstein frame taking these factors into account and presents some preliminary results using dual phase structural steel samples at temperatures up to and exceeding the Curie point.

2. Methodology and design constraints

A major requirement when designing the measurement equipment was that the Epstein frame should fit inside the austenitic steel furnace annealing box made available for the tests, measuring 380 × 280 × 200 mm. Sufficient clearance between the frame and the box, to insure that the induced eddy current in the austenitic box do not influence the magnetic measurements, is also required. Taking these factors into account, the design shown in figure 1 was decided on. The design is as large as can be accommodated by the annealing box while allowing a minimum of 20 mm clearance between the coils and the box on all sides. The frame is designed to accommodate smaller samples than mandated by IEC standards, measuring 200 mm × 20 mm × sample thickness. The annealing box is equipped with a gas feed to supply argon gas during the tests to minimise oxidation of both the samples and wires making up the primary and secondary coils. A 10 mm diameter tube leading from the interior of the box to the exterior of the furnace is also included to allow the wires from the frame to exit the furnace without being exposed to the furnace atmosphere.

In order to accurately characterise the structural steels of interest it is necessary to employ low frequency (≤ 1 Hz) excitation to minimise the influence eddy currents, along with a relatively high applied field. This leads to a requirement to develop a frame with a much higher primary coil turns density than most of the previous work in this area [10–15, 22]. These requirements are problematic for the selection of appropriate wire for the apparatus. For the design shown in figure 1, it was

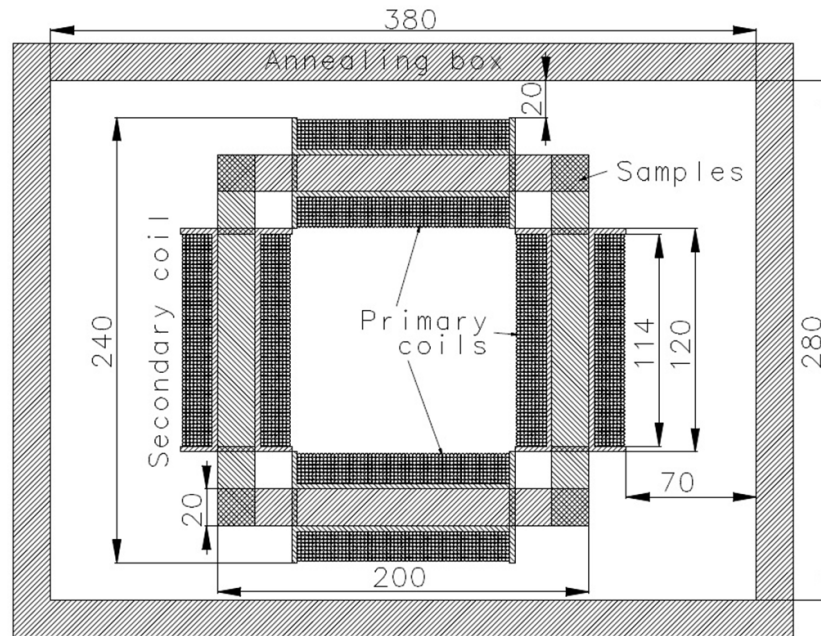


Figure 1. Plan view of high temperature Epstein frame positioned in annealing box. Dimensions in mm.

Table 1. Electrical properties of wires at high temperatures.

Material	Melting point (°C)	Temp. coef. of resistance ($\Omega s \Omega^{-1} \text{ } ^\circ\text{C}^{-1}$)	Resistivity coef. ($\Omega \text{ m}^2 \text{ m}^{-1}$)	Resistance of 87 m of 1 mm $\text{ } \varnothing$ wire at		Maximum current at 800 °C (A)	Maximum applied field at 800 °C (kA m^{-1})
				20 °C (Ω)	800 °C (Ω)		
Copper	1083	4×10^{-3}	1.724×10^{-8}	2.5	9.6	1.04	1.83
Copper, 27% Ni clad	1100	3×10^{-3}	2.33×10^{-8}	3.3	10.5	0.95	1.67
Silver	951	6.1×10^{-3}	1.59×10^{-8}	2.3	12.4	0.81	1.42
Tungsten	3422	4.5×10^{-3}	5.65×10^{-8}	8.1	34.5	0.29	0.51
Molybdenum	2623	4.58×10^{-3}	5.20×10^{-8}	7.5	32.2	0.31	0.55
Tantalum	3017	3.8×10^{-3}	12.4×10^{-8}	17.6	66.6	0.15	0.26

determined that the coil formers could accommodate 600 turns of 1 mm diameter wire with insulation. At an average coil diameter of 40 mm, with 2 m lead wires, just over 87 m of wire is required. Wire made from specialist high temperature materials is available; the melting points of molybdenum, tantalum and tungsten are all in excess of 2500 °C, as shown in table 1. Disregarding the high price, these make for attractive selections for the construction of a robust high temperature test rig. However, the high resistance of these materials, especially at high temperatures means that, using the equipment available for these tests with a fixed maximum applied voltage of 10 V, the maximum applied field would be below the coercive field for most structural steels, even at room temperature, thus the test would not give the ‘true’ full magnetic properties of the materials of interest.

Previous high temperature frames [15] have employed nickel coated copper wire in order to prevent oxidation of the wire. Although nickel coated copper offers performance in terms of resistivity which is almost equivalent to copper wire (see table 1), the ferromagnetic nickel coating introduces additional measurement uncertainties. As the apparatus described here is designed to be used in an inert

atmosphere, the additional protection from oxidation was deemed unnecessary. After taking factors of performance, cost, availability, etc into account, silver plated copper wire was chosen as a material which would mean that the magnetic properties of interest could be measured, albeit with the risk of the wire failing at higher temperatures due to thermal softening.

As shown in table 1 in order to apply a field of 1.83 kA m^{-1} at 800 °C, 200 windings per coil is needed. Tests during the development of the equipment employed concentrically wound primary (200 turn) and secondary (100 turn) coils. The diameter of the wire and the size of the coil formers meant that it was necessary to tightly wind the coils, resulting in a number of wire failures in the inner windings at higher temperatures. The exact cause of failure is not certain, but it seems likely that the wire tension coupled with the thermal softening of the wire resulted in failure through creep mechanisms. For this reason, a simplified coil configuration was employed, featuring four identical 200 turn coils. Three of these coils are wound in series to provide excitation (primary coils) and one is used to measure the flux density (secondary coil).

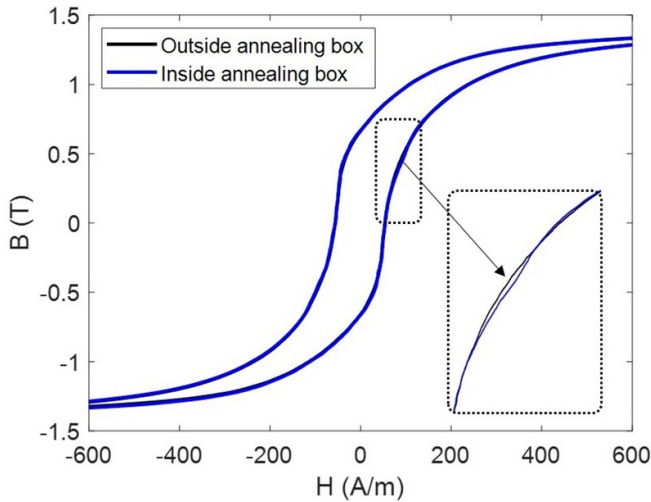


Figure 2. Comparison of silicon steel BH loops with Epstein frame inside and outside austenitic annealing box.

The value of the applied field (H) and the flux density (B) are calculated from the current applied to the primary coils and voltage over the secondary coil respectively according to procedures widely reported elsewhere [8, 9]. IEC standards [8] dictate that a mutual inductor should be used to eliminate the error due to the air flux introduced by the difference in area between the sample and secondary winding. An estimation of this error is given by:

$$B_{\text{meas}} - B_{\text{sample}} = \mu_0 H_{\text{max}} \frac{S_{\text{tot}} - S}{S}$$

where $B_{\text{meas}}(T)$ is the magnetic flux measured by the secondary winding, $B_{\text{sample}}(T)$ is the magnetic flux in the sample, μ_0 is the permeability of free space, H_{max} (A m^{-1}) is the value of the applied field, S_{tot} is the cross sectional area of the secondary coil (m^2) and S is the area of the sample (m^2) [8, 15]. For the system described here, the maximum error has been calculated to be less than 2%, so for these tests the influence of air flux has been disregarded.

Another potential source of error is the proximity of the austenitic furnace annealing box to the coils in the frame. This was set at a minimum of 20 mm at the design stage (see figure 1). A test was set up to verify if this clearance is sufficient, with BH loops measured with the Epstein frame positioned outside and inside the annealing box using 3.5 wt% Si M270 grade silicon steel samples supplied by Cogent Power. The results of the test are shown in figure 2. It can be seen from the plot that the difference between the two measurements is very small, well below the noise floor for the system.

3. FEM validation of proposed design

3D finite element models were developed using COMSOL Multiphysics to verify the simplified coil configuration described in this paper (three primary/one secondary, shown in figure 1) in comparison with the standard Epstein frame (four

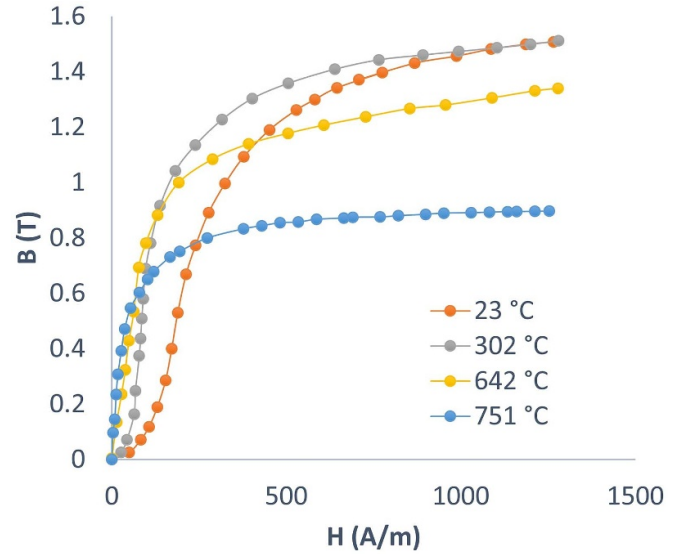


Figure 3. BH curve for a pure iron sample at different temperatures, data replotted from [20].

primary/four secondary coils [8]) across the required temperature range. The geometry of the samples and coil setup are the same as described earlier in this section and shown in figure 1. The initial magnetisation curves used as inputs to the models are taken from published literature [20] reporting BH characteristics measured on a toroidal pure iron sample (Rowland ring: external diameter 3.5 cm, internal diameter 3 cm, height 0.4 cm) at different temperatures and are replotted in figure 3.

The modelled magnetic flux density distribution in the samples for the four primary/four secondary and the three primary/one secondary coil configurations are shown in figures 4(a) and (b), respectively. Flux distributions are shown for a temperature of 23 °C at peak excitation current. As might be expected, figure 4(a), showing the standard Epstein frame configuration with a primary coil on each leg of the frame has a reasonably uniform magnetic flux distribution for the volume of sample under all the concentrically wound secondary coils. It can be seen from figure 4(b) that for the three primary/one secondary coil configuration, the flux density in the volume under the secondary coil is slightly lower than the flux density in the volume under the primary coils due to flux leakage.

Figure 4 shows the model output BH curves from the two coil configurations at temperatures from 23 °C (figure 5(a)) to 751 °C (figure 5(d)). In both cases the flux density is calculated from the volume underneath the secondary coils. It can be seen from the plots that at low applied fields ($<200 \text{ A m}^{-1}$), the difference between the three and four primary coil design is small, decreasing from 82 mT (23 °C) to 55 mT (751 °C) at 200 A m^{-1} . At higher applied fields ($>200 \text{ A m}^{-1}$), the difference in the flux density becomes larger, decreasing from 190 mT (23 °C) to 85 mT (751 °C) at 800 A m^{-1} . The largest difference in flux density between the two coil configurations is 14.2% at 23 °C (at maximum flux density). The maximum difference in flux density reduces to around 10% as the temperature increases to 751 °C. Results show that

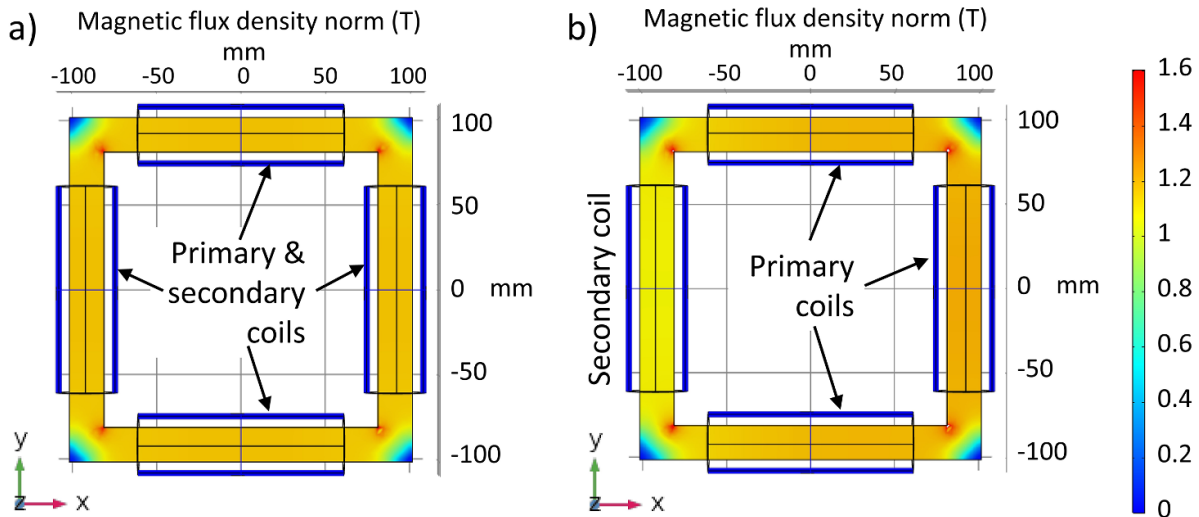


Figure 4. Magnetic flux density distribution in two different Epstein frame configurations; (a) four primary/four secondary coils; (b) three primary/one secondary coil.

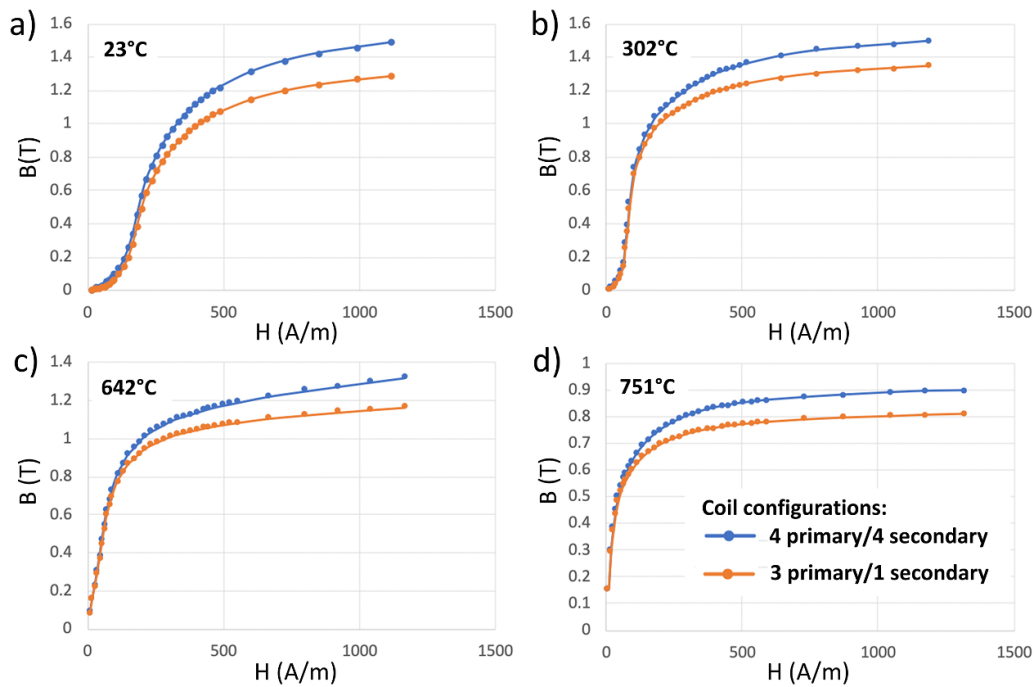


Figure 5. Comparison of model output BH curves from three and four primary coil Epstein frame configurations at; (a) 23 °C, (b) 302 °C, (c) 642 °C, and (d) 751 °C.

although the simplified three primary/one secondary coil configuration does result in some measurement error, especially at higher flux densities, errors are predictable and systematic and decrease as temperature increases.

Figure 6 shows BH loops measured at room temperature using the three primary/one secondary coil configuration and a Brockhaus Epstein frame constructed according to IEC 60404-2, driven by an MPG 200 Brockhaus Electrical Steel Tester. The samples used in this test were 3.5 wt% Si M270 grade silicon steel supplied by Cogent Power, cut to IEC standards for the Brockhaus tester and 200 × 20 mm for the high temperature frame. As predicted by the room temperature FEM

simulation shown in figure 5(a), there is very little difference between the two plots at low applied fields but at higher fields the difference in flux density increases, resulting in difference of 13.8% at 1500 A m⁻¹, very close to the maximum error of 14.2% predicted by the model.

4. Construction of high temperature Epstein frame

Figure 7(a) shows a single coil former for the frame. The coil former is constructed from 120 mm sections of 30 mm diameter aluminium oxide tube with aluminium nitride flanges

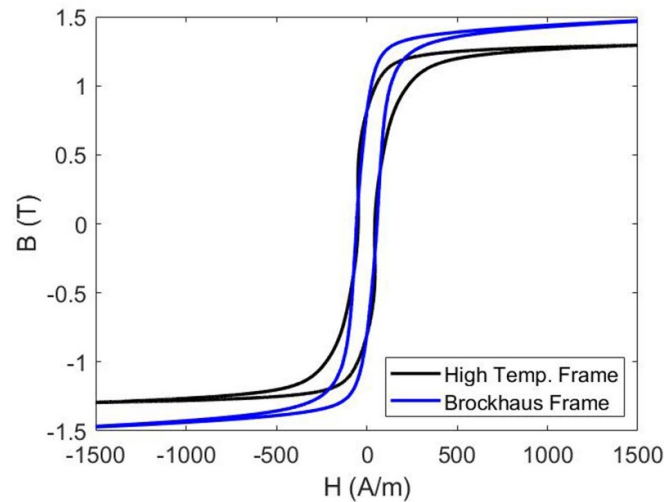


Figure 6. Comparison of silicon steel BH loops from high temperature Epstein frame and commercial Epstein frame.

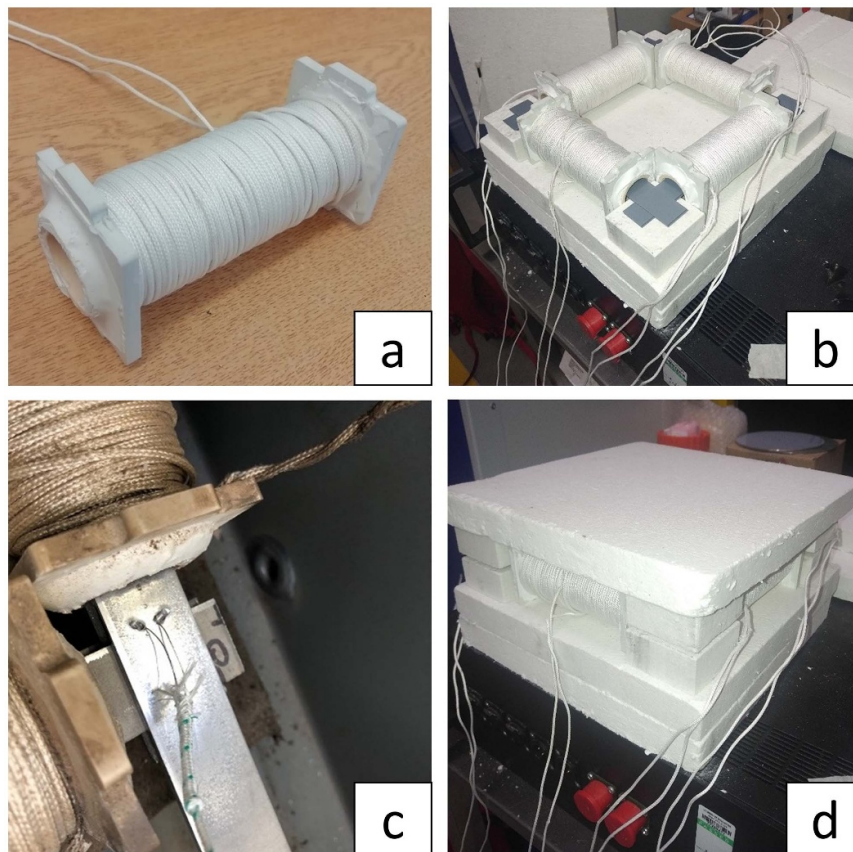


Figure 7. Construction of high temperature Epstein frame: (a) a single coil, (b) Epstein frame with layered samples inserted, (c) thermocouple wire bonded to sample, (d) complete Epstein frame layered with Vitcas insulation boards.

attached. The tubes and flanges are bonded together with a high temperature adhesive. The coil formers are wound with 200 turns of silver plated copper wire sleeved with insulation. The insulating sleeving is 70% alumina, 30% silica and has a maximum temperature of 1200 °C. The sleeving is used primarily as an electrical insulator between the windings of the coils. It is relatively thin, resulting in an overall diameter of

around 2 mm when used with 1 mm diameter wire; an important factor considering the relatively high turns density required for this design. Previous unsuccessful tests had shown that tight winding of the coils can result in failure of the internal windings so the coil windings were kept loose, with winding layers separated by layers of high temperature ceramic tape.

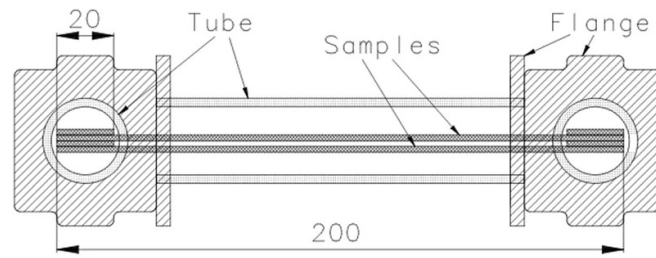


Figure 8. Side view of arrangement of samples in Epstein frame. Dimensions in mm.

Figure 7(b) shows the four coils configured as an Epstein frame with the samples inserted on each side. Samples are supported by blocks of Vitcas insulation, with the samples positioned in the centre of the coils. Thermocouple wire was bonded to one of the samples, as shown in figure 7(c) to monitor the sample temperature during the tests. The wires are positioned to measure the temperature at the centre of the sample. Figure 7(d) shows the Epstein frame layered with sheets of insulation. The two layers of insulation on the bottom provide 50 mm clearance between the bottom of the frame and the bottom of the annealing box. There is one layer of insulation on the top of the frame. Two bricks were placed on this to hold the samples in place during the tests.

5. Test set-up

A commercial grade dual phase steel (DP600: 0.17 wt% C, 1.5–2.2 wt% Mn) supplied by Tata Steel, Europe was selected for the tests. The material was cut into $200 \times 20 \times 2$ mm pieces, with two pieces per side arranged as shown in figure 8. When the samples were in-situ in the annealing box, the samples were weighted down in the corners to help prevent movement during the tests. The annealing box was provided with a constant flow of argon gas at a flow rate of $400 \text{ cm}^3 \text{ min}^{-1}$ throughout the test to prevent oxidation. The furnace was set at a heating rate of $20 \text{ }^\circ\text{C}$ per minute with the temperature controlled by the sample thermocouple. The actual heating rate as measured by the thermocouple did not exceed $10 \text{ }^\circ\text{C}$ per minute and was much slower approaching the Curie temperature. A maximum temperature of $783 \text{ }^\circ\text{C}$ was reached during the test.

Data was acquired from the secondary coil and a current sense resistor wired in series with the primary coil for 1 min at 2 min intervals. A 1 Hz sinusoidal excitation waveform was used in the tests, with 50 repetitions averaged for each measurement to reduce noise. Data was acquired during the heating and cooling stages.

6. Results and discussion

Figure 9 shows BH loops at selected temperatures during heating (figures 9(a) and (b)) and cooling (figures 9(c) and (d)). The dominant effect of heating up to around $600 \text{ }^\circ\text{C}$ (figure 9(a)) is a narrowing of the loop as the coercive field decreases along

with a large decrease in the maximum H value. The reduction in the maximum H value is due to the nature of the excitation electronics. A fixed voltage is applied and as the resistance of the wire increases with increasing temperature, the current through the primary coils decreases reducing the amplitude of the applied field. As the temperature exceeds around $600 \text{ }^\circ\text{C}$ the nature of the change in the BH loops is very different. There is a rapid decrease in flux density (B) as the temperature approaches the Curie point and the samples become paramagnetic. At $783 \text{ }^\circ\text{C}$ the flux density reduces to near zero. The change in the loops on cooling (figures 9(c) and (d)) follow a similar trend to those during the heating stage.

Figure 10 shows two magnetic parameters extracted from the BH loops shown in figure 9; coercivity (figure 10(a)) and maximum permeability (figure 10(b)). These were selected as representative of the magnetic parameters of interest for high temperature steel processing applications [1–7], rather than the usual power loss measurements of interest to Epstein frame users looking at electrical steels at power frequencies. It should be noted that due to the reduction in maximum H values with temperature, there will be some distortion of these magnetic parameters. These plots are not presented as absolute magnetic measurements, rather as an illustration of the capabilities of the developed system.

It can be seen from figure 10 that the coercivity and permeability plots follow somewhat different paths during heating and cooling. Intuitively, it might be expected that the changes in these parameters would be symmetrical, but this discrepancy can be explained in terms of the changes in material microstructure at different stages of the test. The chemical composition of the DP 600 sample has 0.17 wt% C. The starting microstructure before the annealing test is around 20% martensite and 80% ferrite. Upon heating, the martensite phase within the microstructure is tempered and an increase in permeability is expected. When the temperature reaches its highest point, $783 \text{ }^\circ\text{C}$, about 71% of the ferromagnetic phases have transformed into austenite (paramagnetic, permeability = 1), hence a lower permeability is expected at this point. Upon cooling, the austenite phase will transform back into ferromagnetic phases, with a final microstructure phase mix of 80% ferrite and 20% pearlite expected at room temperature. The non-equilibrium heating and cooling means the transformation temperature to austenite on heating is higher than the transformation temperature back from austenite to a ferromagnetic phase on cooling, this and the different second

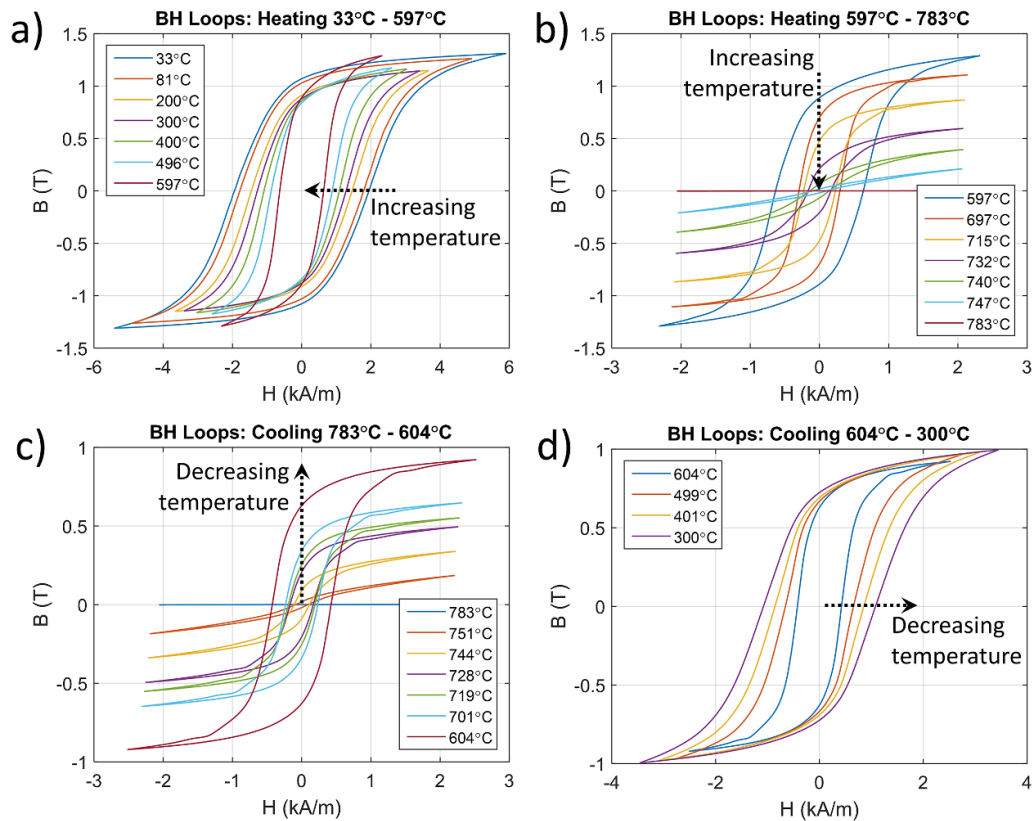


Figure 9. BH loops measured during heating and cooling: (a) heating from 33 °C to 597 °C, (b) heating from 597 °C to 783 °C, (c) cooling from 783 °C to 604 °C, (d) cooling from 604 °C to 300 °C.

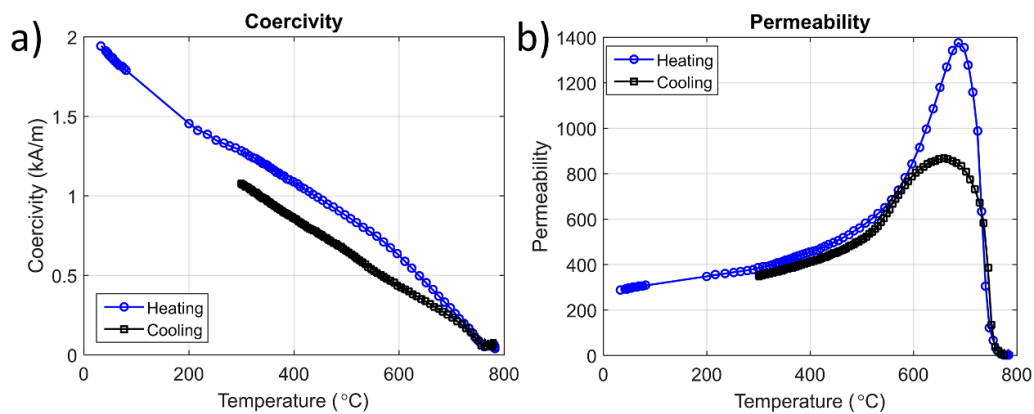


Figure 10. Parameters extracted from BH loops measured during heating and cooling: (a) coercivity and (b) maximum permeability.

phases (pearlite compared to tempered martensite) mean that there is a lower maximum permeability value during the cooling stage.

7. Conclusions

This paper details the development of an Epstein frame designed to measure the magnetic properties of structural steels at temperatures up to the Curie point. A simplified coil configuration has been developed to deal with some of the practical limitations presented by design constraints for the

equipment. The design is validated through finite element modelling which shows that although the simplified configuration does introduce some error to the B component of the measurements, especially at higher flux densities, errors are predictable and systematic with scope for error correction in future implementations of the equipment. To test the developed Epstein frame, BH loops are measured for dual phase steel samples heated to 783 °C. Coercivity and permeability values are extracted from the loops and correlated with microstructural changes in the material. The results of the test show that accurate BH measurements up to the Curie point are possible using the novel coil configuration.

Future work will be geared towards the generation of data sets of full magnetic parameters (BH loop, permeability, coercivity, remanence, saturation magnetisation, etc) for a range of Advanced High Strength Steels up to the Curie temperature. These data sets will inform the development and refinement of online monitoring systems for high temperature steel strip manufacture, feeding into forward models of magnetic properties, model inversion for property characterisation and interpretation of real world data.

Data availability statement

The data that support the findings of this study are available upon reasonable request from the authors.

Acknowledgment

The authors wish to thank Dr Mohsen Aghadavoudi Jolfaei and Mr Fanfu Wu at the University of Warwick for help with experimental procedures, Dr Frenk Van Den Berg at Tata Steel for advice on the construction of the high temperature Epstein fame and the Steel Processing Group from Warwick Manufacturing Group (WGM), University of Warwick, for the provision of facilities and equipment. The work was supported by the ‘Online Microstructure Analytics (OMA)’ project funded by the European Commission under the Research Fund for Coal and Steel (Grant Agreement No. 847296) and the Engineering and Physical Sciences Research Council under Grants RIME (EP/P027210/01) and SUSTAIN (EP/S018107/1).

ORCID iD

John W Wilson  <https://orcid.org/0000-0003-2139-1250>

References

- [1] Kopineck H-J, Löffel R and Otten H-B 1993 Industrial on-line texture determination in rolled steel strips *J. Nondestruct. Eval.* **12** 13–9
- [2] Hutchinson B, Moss B, Smith A, Astill A, Scruby C, Engberg G and Björklund J 2002 Online characterisation of steel structures in hot strip mill using laser ultrasonic measurements *Ironmak. Steelmak.* **29** 77–80
- [3] Ph Papaelias M, Strangwood M, Peyton A J and Davis C L 2004 Measurement and modeling of the electromagnetic response to phase transformation in steels *Metall. Mater. Trans. A* **35** 965–72
- [4] Shen J, Zhou L, Jacobs W, Hunt P and Davis C 2019 Real-time in-line steel microstructure control through magnetic properties using an EM sensor *J. Magn. Magn. Mater.* **490** 165504
- [5] Yang H *et al* 2019 EM sensor array system and performance evaluation for in-line measurement of phase transformation in steel *Insight, Non-Destr. Test. Cond. Monit.* **61** 153–7
- [6] Skarlatos A, Reboud C, Svaton T, de Guereau A M, Kebe T and Van-Den-Berg F 2016 Modelling the impoc response for different steel strips *Proc. 19th Conf. on Non-Destructive Testing WCNDT* vol 6 p 22
- [7] Peyton A J *et al* 2016 The application of electromagnetic measurements for the assessment of skin passed steel samples *WCNDT-2016* p Th_2_1_4
- [8] International Electrotechnical Commission 2008 Magnetic materials—part 2: methods of measurement of the magnetic properties of electrical steel strip and sheet by means of an Epstein frame
- [9] Fiorillo F 2010 Measurements of magnetic materials *Metrologia* **47** S114
- [10] Foster K 1986 Temperature dependence of loss separation measurements for oriented silicon steels *IEEE Trans. Magn.* **22** 49–53
- [11] Messal O, Sixdenier F, Morel L and Burais N 2012 Temperature dependent extension of the Jiles-Atherton model: study of the variation of microstructural hysteresis parameters *IEEE Trans. Magn.* **48** 2567–72
- [12] Mouillet A, Ille J L, Akroune M and Dami M A 1994 Magnetic and loss characteristics of nonoriented silicon-iron under unconventional conditions *IEE Proc., Sci. Meas. Technol.* **141** 75–8
- [13] Akroune M, Aouli R, Dami M A and Mouillet A 1996 Characterisation of nonoriented electric alloys under nonconventional conditions *IEE Proc., Sci. Meas. Technol.* **143** 35–40
- [14] Cheng Z *et al* 2013 Modeling of magnetic properties of GO electrical steel based on Epstein combination and loss data weighted processing *IEEE Trans. Magn.* **50** 1–9
- [15] Ababsa M L, Ninet O, Velu G and Lecointe J P 2018 High-temperature magnetic characterization using an adapted Epstein frame *IEEE Trans. Magn.* **54** 1–6
- [16] Boehm A and Hahn I 2014 Measurement of magnetic properties of steel at high temperatures *IECON 2014-40th Conf. IEEE Industrial Electronics Society (IEEE)* pp 715–21
- [17] Takahashi N, Morishita M, Miyagi D and Nakano M 2010 Examination of magnetic properties of magnetic materials at high temperature using a ring specimen *IEEE Trans. Magn.* **46** 548–51
- [18] Takeuchi H, Yogo Y, Hattori T, Tajima T and Ishikawa T 2017 High-temperature magnetization characteristics of steels *ISIJ Int.* **57** 1883–6
- [19] Cedillo E, Ocampo J, Rivera V and Valenzuela R 1980 An apparatus for the measurement of initial magnetic permeability as a function of temperature *J. Phys. E* **13** 383–6
- [20] Bozorth R M 1993 *Ferromagnetism* (New York: Wiley) p 992
- [21] Di Barba P and Savini A 2000 *Non-Linear Electromagnetic Systems: ISEM '99* vol 18 (Amsterdam: IOS Press)
- [22] Hussain S, Benabou A, Clénet S and Lowther D A 2018 Temperature dependence in the Jiles–Atherton model for non-oriented electrical steels: an engineering approach *IEEE Trans. Magn.* **54** 1–5